EUROPEAN ORGANIZATION FOR NUCLEAR RESEARCH

CERN-EP/83-49
6 April 1983

EXPERIMENTAL STUDY OF x-DISTRIBUTIONS IN SEMILEPTONIC NEUTRAL-CURRENT NEUTRINO REACTIONS

CHARM Collaboration

M. Jonker[1] and F. Udo
NIKHEF, Amsterdam, The Netherlands

J.V. Allaby, U. Amaldi, C. Barbiellini[2], A. Capone, W. Flegel,
W. Kozanecki[3], K.H. Mess[4], M. Metcalf, J. Meyer[4], R.S. Orr[5],
J. Panman, A.M. Wetherell and K. Winter
CERN, Geneva, Switzerland

V. Blobel, F.W. Büsser, P.D. Gall, H. Grote, B. Kröger, E. Metz,
F. Niebergall, K.H. Ranitzsch and P. Stähelin
II. Institut für Experimentalphysik*), Universität Hamburg,
Hamburg, Fed. Rep. of Germany

P. Gorbunov, E. Grigoriev, V. Kaftanov, V. Khovansky and A. Rozanov
Institute of Theoretical and Experimental Physics, Moscow, USSR

A. Baroncelli[6], B. Borgia[7], C. Bosio[6], F. Ferroni[7], E. Longo[7],
P. Monacelli[7], F. de Notaristefani[7], P. Pistilli[7],
C. Santoni[6] and V. Valente[8]
Istituto Nazionale di Fisica Nucleare, Rome, Italy

(Submitted to Physics Letters)

---

1) Now at SLAC, Stanford, Calif., USA.
2) On leave of absence from the Latoratori Nazionali dell'INFN, Frascati, Italy.
3) Now at University of California, Riverside, Calif., USA.
4) Now at DESY, Hamburg, Fed. Rep. of Germany.
5) Now at University of Toronto, Ontario, Canada.
6) INFN Sez. Sanità and Istituto Superiore di Sanità, Rome, Italy.
7) Istituto di Fisica, Università di Roma, and INFN, Sez. di Roma, Rome, Italy.
8) Laboratori Nazionali dell'INFN, Frascati, Italy.

*) Supported by the Bundesministerium für Forschung und Technologie, Bonn,
Fed. Rep. of Germany.

ABSTRACT

Neutral-current differential cross-sections as a function of the scaling variable x for deep inelastic neutrino- and antineutrino-nucleon scattering on an isoscalar target were measured in the CERN SPS 200 GeV/c Narrow-Band Beam with the CHARM fine-grained calorimeter.

The data have been corrected for the experimental resolutions using a novel unfolding procedure. Its validity is tested on charged-current reactions.

The x-distributions determined in neutral-current reactions are found to be compatible with the results obtained in charged-current reactions, as expected by the quark model of the nucleon and by the standard model of the weak interactions.

Extensive studies of x-distributions and structure functions in deep inelastic neutrino- and antineutrino-nucleon charged-current (CC) interactions

$$\overset{(-)}{\nu}_{\mu} + N \rightarrow \mu^{\mp} + X$$

have revealed many details of the structure of the nucleons. Several other groups [1-3] as well as the CHARM Collaboration [4] have published data on the structure functions F_2 and xF_3 and their Q^2-dependence.

In neutral-current (NC) interactions

$$\overset{(-)}{\nu}_{\mu} + N \rightarrow \overset{(-)}{\nu}_{\mu} + X$$

the experimental situation is much more difficult than in CC reactions because the outgoing neutrino cannot be detected, and all information has to be gained from the hadronic final state X and from the beam properties. It is therefore not surprising that much less is known on structure functions for NC interactions. Only one bubble-chamber experiment [5] has reported a measurement of a NC x-distribution in a low-energy (10 GeV) neutrino beam and with low statistics (23 events).

The aim of this experiment was to measure x-distributions for NC neutrino and antineutrino interactions at high energies with good statistics.

The differential NC cross-section is parametrized directly in terms of the quark distributions. With the valence quark distribution $q_{val}(x)$ and assuming a symmetrical sea-quark distribution $q_{sea}(x) = \bar{q}_{sea}(x)$ and $u_{sea}(s) + c_{sea}(x) = d_{sea}(x) + s_{sea}(x)$ the cross-sections read:

$$\frac{d\sigma^{NC}}{dxdy} = \frac{G^2 m_p E_\nu}{2\pi} \left[2(u_L^2+d_L^2) + 2(1-y)^2(u_R^2+d_R^2)\right] q_{val}(x,Q^2) + \left[1 + (1-y)^2\right] (u_L^2+u_R^2+d_L^2+d_R^2)\ 2q_{sea}(x,Q^2) \qquad (1a)$$

for neutrinos, and

$$\frac{d\sigma^{NC}}{dxdy} = \frac{G^2 m_p E_\nu}{2\pi} \left[2(1-y)^2(u_L^2+d_L^2) + 2(u_R^2+d_R^2)\right] q_{val}(x,Q^2) + \left[1 + (1-y)^2\right] (u_L^2+u_R^2+d_L^2+d_R^2)\ 2q_{sea}(x,Q^2) \qquad (1b)$$

for antineutrinos.

The corrections to these cross-sections due to asymmetric strange- and charm-quark contributions are small compared to the experimental uncertainties and have been neglected.

The scaling variables x and y are defined by

$$y = \frac{E_h - m}{E_\nu} , \quad x = \frac{Q^2}{2m(E_h - m)} ,$$

where E_ν and E_h are the energy of the neutrino and of the hadronic system, and m stands for the nucleon mass. The NC coupling constants of the left- and right-handed u and d quarks, u_L, u_R, d_L, and d_R, depend in the standard model of electroweak interactions on the value of the electroweak mixing angle only.

For NC events, we measure the energy E_h and the angle θ_h of the hadronic system, and the position of the interaction vertex. In terms of E_h and θ_h the scaling variable x is given by

$$x = \frac{E_\nu (E_h - m) \sin^2 \theta_h}{2m(E_\nu \cos^2 \theta_h - E_h + m)} .$$

The evaluation of x requires knowledge of the initial neutrino energy E_ν. The CERN 200 GeV/c Narrow-Band Beam (NBB) provides a well-defined relationship between the neutrino energy and the distance r of the interaction vertex from the beam axis, up to the inherent beam momentum spread, and the ambiguity between the neutrinos from pion and kaon decay. Owing to these basic limitations and to the experimental resolutions, especially in the angle θ_h, a complete reconstruction of the kinematics on an event-by-event basis is not possible. Therefore we unfolded the measured event distribution to determine the x-distribution which gives the best fit. This approach is in analogy to that we used to obtain the NC y-distributions [6].

In order to test the unfolding procedure CC events were analysed with the same method. For this test we neglected the muon momentum and direction measurements and used only the information available in NC events: hadron energy E_h, hadron angle θ_h, and the vertex position measured by the origin of the hadron shower. The results of the unfolding were then compared with the results of the

standard CC analysis, where all available information was used including the muon momentum, the muon direction, and the vertex determined by the muon track.

The data presented here were obtained with the CHARM neutrino detector in the CERN 200 GeV/c NBB. The NBB selects and focuses pions and kaons produced by the interactions of 400 GeV/c protons on a beryllium target, into a nearly parallel beam with well-defined momentum. Neutrinos are produced by π and K decays in a 300 m long decay tunnel. The dominant decay processes are two-body decays. Together with the small divergence and small momentum spread of the secondary beam this produces a correlation between the neutrino energy and the radial distance r of an interaction from the beam axis (for more details, see ref [6]). The neutrino energy spectrum $\phi(E_\nu,r)$ at a given radius depends only on the production spectra of pions and kaons, and on the characteristics of the magnetic focusing channel and the decay tunnel, and can be reliably calculated. The typical beam momentum spread is ±10 GeV/c.

The CHARM fine-grained calorimeter [7] consists of 78 equal subunits of marble plates with scintillators and proportional drift tubes as detector elements. The fine sampling, both longitudinal and perpendicular to the beam axis, allowed the measurement of the total kinetic energy of particle showers down to 2 GeV as well as their origin and direction. An iron-frame magnet surrounds the marble target and a toroidal iron muon spectrometer follows the target part. Both iron magnets are segmented and used as calorimeters. They are equipped with proportional drift tubes to allow the reconstruction of muon tracks and the measurement of the energy of hadronic showers in these regions.

In the CHARM detector the interaction vertex of a hadron shower is measured with a resolution of a few centimetres at 100 GeV. The vertex resolution allows us to make full use of the radial dependence of the neutrino-energy spectrum. The hadron-energy resolution has been measured in a test beam [8] and was found to be

$$\sigma(E_h)/E_h = 0.53/\sqrt{E_h/\mathrm{GeV}}$$

The unfolding of the x-distribution requires precise knowledge of the angular resolution and its energy- and angle-dependence. Measurements in a pion test beam

at various energies [8] provided some data on the resolution and its energy dependence, but only a small angle range was available. Therefore these measurements had to be supplemented using CC events, which cover the whole energy and angle range of neutrino-induced showers. With these events the measured θ_h was compared with the hadron angle predicted from the measurement of p_μ, θ_μ, and E_h. From this analysis the resolution functions for the "scaled hadron angle" $u = \sqrt{E_h/(2m_p)}\ \theta_h$ were obtained as a function of the hadronic energy E_h. In the small-angle approximation u is related to x and y by $u \sim \sqrt{x(1-y)}$. The energy dependence of the resolution in u is much weaker than that of the resolution in the angle θ_h.

The event-selection criteria have been described elsewhere [9]. The CC events are distinguished from the NC events by the presence of a muon track originating at the shower vertex. The hadron-energy and fiducial-volume cuts were selected to ensure a good signal/background ratio, good event discrimination, and acceptable resolutions without undue loss of event statistics. Only events within 120 cm radial distance from the beam axis for neutrinos and within 90 cm for antineutrinos were accepted. The longitudinal fiducial-volume cut accepted events which had their interaction vertex between subunits 7 and 60, resulting in a fiducial mass of 65 t for neutrinos and 37 t for antineutrinos. A hadronic energy of at least 4 GeV was required to ensure adequate resolutions in all three kinematical observables.

Corrections had to be taken into account for beam background and for event misidentification. Beam background is produced by the following sources:

i) Neutrinos produced in K or π decays which occurred before the momentum selection slits in the beam line ("wide-band background").

ii) Electron neutrinos produced by K_{e3} decays. Both their CC and NC interactions are classified as ν_μ NC reactions and have to be subtracted from the NC event rates.

Event misidentification has two main causes:

i) Muons originating from the decay of pions and kaons within the hadronic shower of a NC event can produce tracks which satisfy the selection criteria for a CC event.

ii) Muons from CC events may leave the detector before being identified or they may be obscured by the hadronic shower. Such events are then classified as NC reactions.

The evaluation of these backgrounds has been described elsewhere [9]. Table 1 summarizes the number of events and the various backgrounds. Corrections for background, event misidentification, and acceptance are included in the unfolding procedure described below.

Our aim is to obtain the x-distributions

$$F_+^{NC} = \left[2(u_L^2+d_L^2) + \frac{2}{3}(u_R^2+d_R)^2\right] q_{val}(x) + \frac{8}{3}(u_L^2+u_R^2+d_L^2+d_R^2)\, q_{sea}(x)$$
$$F_-^{NC} = \left[\frac{2}{3}(u_L^2+d_L^2) + 2(u_R^2+d_R^2)\right] q_{val}(x) + \frac{8}{3}(u_L^2+u_R^2+d_L^2+d_R^2)\, q_{sea}(x) \qquad (2)$$

from the data (the + and - signs denote ν and $\bar{\nu}$ distributions).

The expected event distribution $G(E_h,\theta_h,r)$ in the measured variables can be calculated for a given function $F_\pm(x)$ by folding $F_\pm(x)$ with a beam flux $\phi(E_\nu,r)$, the y-dependence of the reaction, and the known resolution functions for the measured variables, adding the distribution $G^b(E_h,\theta_h,r)$ of background and misidentified events. This can be written formally as:

$$G(E_h,\theta_h,r) = \int R(E_h,\theta_h,r;x)\, F_\pm(x)\, dx + G^b(E_h,\theta_h,r)\ , \qquad (3)$$

where $R(E_h,\theta_h,r;x)$ includes the beam flux, the y-dependence, and the resolution functions.

Using the x-distributions $F_\pm^{NC}(x)$ defined above [eqs. (2)], the differential cross-section [eq. (1)] is rewritten for our analysis in the form:

$$\frac{d^2\sigma^{NC}}{dxdy} = \frac{G^2 m_p E_\nu}{2\pi} F_\pm^{NC}(x)\, F_y^{NC}(y|x)\ , \qquad (4)$$

introducing the functions

$$F_y^{NC}(y|x) = \frac{[1+(1-y)^2] \pm B^{NC}(x)\,[1-(1-y)^2]}{\frac{4}{3} \pm \frac{2}{3} B^{NC}(x)}$$

and

$$B^{NC}(x) = \frac{\left[(u_L^2+d_L^2) - (u_R^2+d_R^2)\right] q_{val}(x)}{\left[(u_L^2+u_R^2) + (d_L^2+d_R^2)\right]\left[q_{val}(x) + 2q_{sea}(x)\right]} .$$

The function $F_y^{NC}(y|x)$, with the property $\int F_y(y)\, dy = 1$, describes for a given value of x the shape of the differential cross-section as a function of y, and is determined by the function $B^{NC}(x)$. For CC reactions, the corresponding function $B^{CC}(x)$,

$$B^{CC}(x) = \frac{q_{val}(x)}{\left[q_{val}(x) + 2q_{sea}(x)\right]}$$

is well known and can be used directly in our analysis of the CC data. For the NC reactions we assume the same ratio of the quark distribution functions and correct for the NC quark couplings according to the standard model of weak interactions. We obtain $B^{NC}(x) = 0.83\ B^{CC}(x)$ for $\sin^2\theta_w = 0.223$ [6].

The assumed parametrization of $F_y^{NC}(y|x)$ does not impose any *a priori* assumption concerning the shape of the function $F_\pm(x)$. We have checked that indeed our results for $F_\pm(x)$ depend only very weakly on the assumed shape of B(x).

The unfolding consists in solving eq. (3) for $F_\pm(x)$, by determining that form of $F_\pm(x)$ which yields the best fit to the measured event distribution. The approach used here was to parametrize the function $F_\pm(x)$ as a linear superposition of bell-shaped functions $b_i(x)$:

$$F_\pm^{NC}(x) = \sum_i a_i b_i(x) , \qquad i = 1...n \tag{5}$$

where a_i are coefficients to be determined. The n functions $b_i(x)$ (we choose n = 7) are quartic B-splines [10], defined between the knots (bins) shown in figs. 1 and 2 and vanish at x = 1. This representation involves no additional *a priori* assumption on the overall shape of $F_\pm(x)$; merely that it varies smoothly over a bin of x.

The linearity of the parametrization allows the expected event distributions $G_i(E_h,\theta_h,r)$ to be calculated for each of the functions $b_i(x)$. The unfolding of the integral equation (3) then consists in determining the coefficients a_i of the

parametrization of $F_{\pm}(x)$ in eq. (5) by a maximum likelihood fit of the linear superposition of the expected event distributions for each of the b_i, $\sum a_i G_i(E_h,\theta_h,r)$, to the experimental distribution. This fit was actually done in the variables $h = \sqrt{E_h}$, u, and r because for h and u the variation of the resolution with hadronic energy is much smaller than for E_h and θ_h.

Using the resulting coefficients a_i, values of $F_{\pm}(x)$, averaged over each bin, are calculated by integrating the parametrization [eq. (5)].

Owing to the finite resolution of the measurement, the statistical fluctuations in the data are magnified by the unfolding procedure, leading to large local fluctuations of the resulting $F_{\pm}(x)$. This fact can also be expressed by the statement that two distributions, differing only in an oscillating function of the type sin (kx) with short period, will, after folding, show only small differences in the distribution of the measured variables. A common method in unfolding procedures [11] is to apply a certain regularization in the fit, in order to reduce the large local fluctuations.

The method adopted in our analysis is to add to the usual likelihood function $L_0(\vec{a})$ a regularizing term $-\tau f_r(\vec{a})$:

$$L_R(\vec{a}) = L_0(\vec{a}) - \tau f_r(\vec{a}) \ , \qquad (6)$$

where $f_r(\vec{a})$ is a sum of terms $(a_{i-1}-2a_i+a_{i+1})^2$ and τ is a weight factor. This has the effect of reducing extremes of local curvature in the resulting function $F_{\pm}(x)$, while leaving the overall shape unchanged. Although the actual value of the weight is somewhat arbitrary, the resulting parameters in a fit of a parametrized expression to the distributions show only small variations if the value of the weight is changed by an order of magnitude in both directions.

Both the CC and NC x-distributions have been obtained in exactly the same way, the secondary muon in CC events being used for event classification only. The statistical errors of the unfolded data were calculated by straightforward error propagation from the statistical errors of the measured data. Owing to the finite experimental resolutions, correlations are introduced between bin contents. Therefore in fitting a theoretical expression to the unfolded distributions the full covariance matrix must be used.

Figures 1 and 2 show the x-distributions $F_{\pm}(x)$ obtained for CC and NC reactions, respectively. The errors plotted correspond to the diagonal elements of the covariance matrix. The CC x-distributions are radiatively corrected. Since the data extend over a wide range in Q^2, we have applied corrections for scaling violations, using our results in CC reactions and assuming that they apply to NC reactions as well. The distributions are projected onto $Q^2 = 5\ GeV^2$ although the correction is small compared to the statistical errors. Figure 3 shows the measured NC distributions in the variables r, h, and u together with the curves representing $\sum a_i G_i(h,u,r)$ as obtained by the fit. The data are well represented by the curves.

Also shown in figs. 1a and 1b are the radiatively-corrected CC x-distributions obtained with the normal analysis, where the muon momentum vector was used to determine the kinematics; for these data the statistical errors are much smaller. The unfolded data agree within errors with the CC data obtained with the momentum analysis, demonstrating the reliability of the method.

More quantitatively we have compared the CC x-distribution obtained with and without using the measurement of the muon momentum vector by fitting them with parametrizations of the quark distribution functions. We expressed the x distributions by the quark functions q_{val} for the valence and q_{sea} for the sea quarks:

$$\begin{aligned} F_+^{CC}(x) &= 2q_{val}(x) + \frac{8}{3} q_{sea}(x) \\ F_-^{CC}(x) &= \frac{2}{3} q_{val}(x) + \frac{8}{3} q_{sea}(x) \ , \end{aligned} \tag{7}$$

using the parametrizations

$$\begin{aligned} q_{val}(x) &= \frac{3}{\beta(a,\ b+1)} x^a (1-x)^b \\ q_{sea}(x) &= C(c+1)(1-x)^c \ . \end{aligned} \tag{8}$$

$\beta(a, b+1)$ is Euler's beta function used for normalization, assuming $\int (q_{val}/x)\, dx = 3$, as predicted by the Gross - Llewellyn Smith sum rule in the context of the quark-parton model of the nucleon. The parameter C is the integral over the sea-quark content of the nucleon and was used to calculate $\bar{q}/(q+\bar{q})$, the relative antiquark content, which is the parameter quoted in table 2.

The parameter c, defining the shape of the sea distribution, was fixed at $c = 6.18$, the value obtained in a fit to the x-distribution (fig. 1) of the normal CC analysis. Owing to the relatively large bin width at small x, the data are not sensitive to this parameter [12].

This parametrization was fitted simultaneously to the neutrino and antineutrino data. The resulting parameters are shown in table 2. The fits are shown as solid curves in figs. 1 and 2. Column (2) in table 2 shows the parameters determined by the fit to the CC data of the normal analysis, where the muon momentum vector was used for determining the kinematics. The resulting parameters for the unfolded CC data and their errors are given in table 2, column (3).

The parameter errors in columns (3) and (4) including uncertainties in the background subtractions and small systematic errors due to the regularization are relevant for the comparison of CC and NC data. Systematic errors due to uncertainties in the overall normalization and in the experimental resolution functions apply to all unfolding results and are given in column (5). Comparing columns (2) and (3) in table 2 for CC data we conclude that reliable x-distributions can be obtained by the unfolding methods developed here, without using the measurement of the muon momentum vector.

For the data on $F_{\pm}^{NC}(x)$ from the NC reactions we performed a fit with the same parametrization for the quark momentum distribution functions as before, taking into account the coupling constants [eq. (2)]. The resulting parameters are given in table 2, column (4). The fitted parameter values agree within errors with the values from the CC reactions. The amount of sea quarks as seen by the neutral and the charged current agrees also with that estimated from our previous analysis [6] of the shape of the NC y-distribution.

To summarize, we have shown that it is possible to determine x-distributions in NC-induced neutrino reactions with the CHARM fine-grained calorimeter using a narrow-band beam by properly unfolding the beam ambiguities and the experimental resolutions. When applied to CC events without using the measurement of the muon momentum vector, results consistent with the standard analysis of these events are

obtained. As predicted by the quark-parton model and by the standard model of weak interactions, no significant difference in the structure of the nucleon is found in NC reactions as compared with CC reactions. To observe the expected small differences between NC and CC x-distributions caused by the different strange- and charm-quark contributions improved resolutions and higher statistics will be needed.

Acknowledgements

We would like to thank most sincerely our many technical collaborators for their competent and enthusiastic help, the members of the SPS staff for the excellent operation of the accelerator, G. Cavallari, H. Heyne, J. May, G. Sigurdsson, and G. Stefanini for their contributions to the beam monitoring, and P. Lazeyras and his group for operating the Narrow-Band Beam. We wish to thank F. Schneider and E. Gygi for their help with the proportional tubes, and J. Audier and M. Busi for their excellent work on data handling.

REFERENCES

[1] P.C. Bosetti et al., BEBC-ABCLOS Collaboration, Nucl. Phys. B142 (1978) 1.

[2] J.G.H. de Groot et al., CDHS Collaboration, Z. Phys. C1 (1979) 143.

[3] H. Wahl, CDHS Collaboration, *in* Proc. 16th Rencontre de Moriond, Les Arcs, 1981 (Ed. Frontières, Dreux, 1981), p. 268.

[4] M. Jonker et al., CHARM Collaboration, Phys. Lett. 109B (1982) 133 and J. Panman, Ph.D. Thesis, University of Amsterdam (1981).
F. Bergsma et al., CHARM Collaboration, Phys. Lett. 123B (1983) 269.

[5] C. Baltay et al., Phys. Rev. Lett. 44 (1980) 916.

[6] M. Jonker et al., CHARM Collaboration, Phys. Lett. 102B (1981) 67.

[7] A.N. Diddens et al., CHARM Collaboration, Nucl. Instrum. Methods 178 (1980) 27.

[8] M. Jonker et al., CHARM Collaboration, Nucl. Instrum. Methods 200 (1982) 183.

[9] M. Jonker et al., CHARM Collaboration, Phys. Lett. 99B (1981) 265.

[10] C. de Boor, A practical guide to splines (Springer, NY, 1978).

[11] See, for example,
B.W. Rust and W.R. Burrus, Mathematical programming and the numerical solution of linear equations (American Elsevier, New York, 1972).
R.S. Anderssen, F.R. de Hoog and M.A. Lukas (eds.), The application and numerical solution of integral equations (Sijtoff and Noordhoff, Alphen aan den Rijn, 1980).
C. Chiaruttini et al., An unfolding procedure for determining the charm fragmentation function from neutrino dimuon data, Contribution to 10th Int. Symposium on Lepton and Photon Interactions at High Energies, Bonn, 1981.

[12] Preliminary results of this analysis were presented at the Neutrino '82 Conference: A. Capone (CHARM Collaboration), Proc. Neutrino '82 Conference, Balatonfüred, Hungary, 1982 (Central Research Institute for Physics, Budapest, 1982), vol. 2, p. 121. The comparison was based on published parameters [4] from a Buras-Gaemers fit to the CC data, with a finer binning in x and without regularization, with a value of $c = 4.55 \pm 0.49$.

Table 1

Event numbers and background with $E_h > 4$ GeV

	ν		$\bar{\nu}$	
	NC	CC	NC	CC
Raw events	2352	6496	1021	2689
K_{e3} - BG	-191	-	-42	-
WBB - BG	-60	-81	-92	-197
CC $\leftrightarrow$ NC	-134	+134	-24	+24
Corrected events	1967	6549	863	2516

Table 2

Quark momentum distribution function parameters for CC and NC reactions using the parametrizations given in the text [eqs. (7) and (8)]. Column (2) gives the CC results using the measurement of the muon momentum vector, and column (3) the CC results from the unfolding method, without using the measurement of the muon momentum vector. Radiative corrections are taken into account. Column (4) gives the result from the unfolding method for NC reactions. The quoted errors include uncertainties in the background subtraction and in the unfolding method. The systematic errors given in column (5) include uncertainties in the normalization and the u-resolution and apply to all unfolding results.

(1)	(2)	(3)	(4)	(5)
Parameter	CC with muon measurement	CC from unfolding	NC from unfolding	Systematic errors
a	0.47 ± 0.02	0.45 ± 0.05	0.44 ± 0.05	±0.05
b	2.71 ± 0.11	2.97 ± 0.16	2.79 ± 0.24	±0.09
$\bar{q}/(q+\bar{q})$	0.14 ± 0.005	0.17 ± 0.03	0.13 ± 0.03	±0.02

Figure captions

Fig. 1 : Charged-current x-distributions $F_+^{CC}(x)$ for neutrino interactions (a) and $F_-^{CC}(x)$ for antineutrino interactions (b), obtained with the method described in the text with corrections for scaling violations and radiative corrections. The solid curves correspond to the structure function fit given in table 2, column (3), the histogram shows the results of the CC analysis using the muon measurement.

Fig. 2 : Neutral-current x-distributions $F_+^{NC}(x)$ for neutrino interactions (a) and $F_-^{NC}(x)$ for antineutrino interactions (b). The solid curves correspond to the fit given in table 2, column (4).

Fig. 3 : Comparison of NC event distributions (ν and $\bar{\nu}$) with the results of the unfolding fit described in the text [eq. (6)]. The histogram shows the measurement, the solid line represents the result of the fit and includes the background event distribution:

a) radial distribution;

b) hadron-energy distribution in bins of $h = \sqrt{E_h}$;

c) "scaled" angular distribution in bins of $u = \sqrt{E_h/(2m_p)}\ \theta_h$.

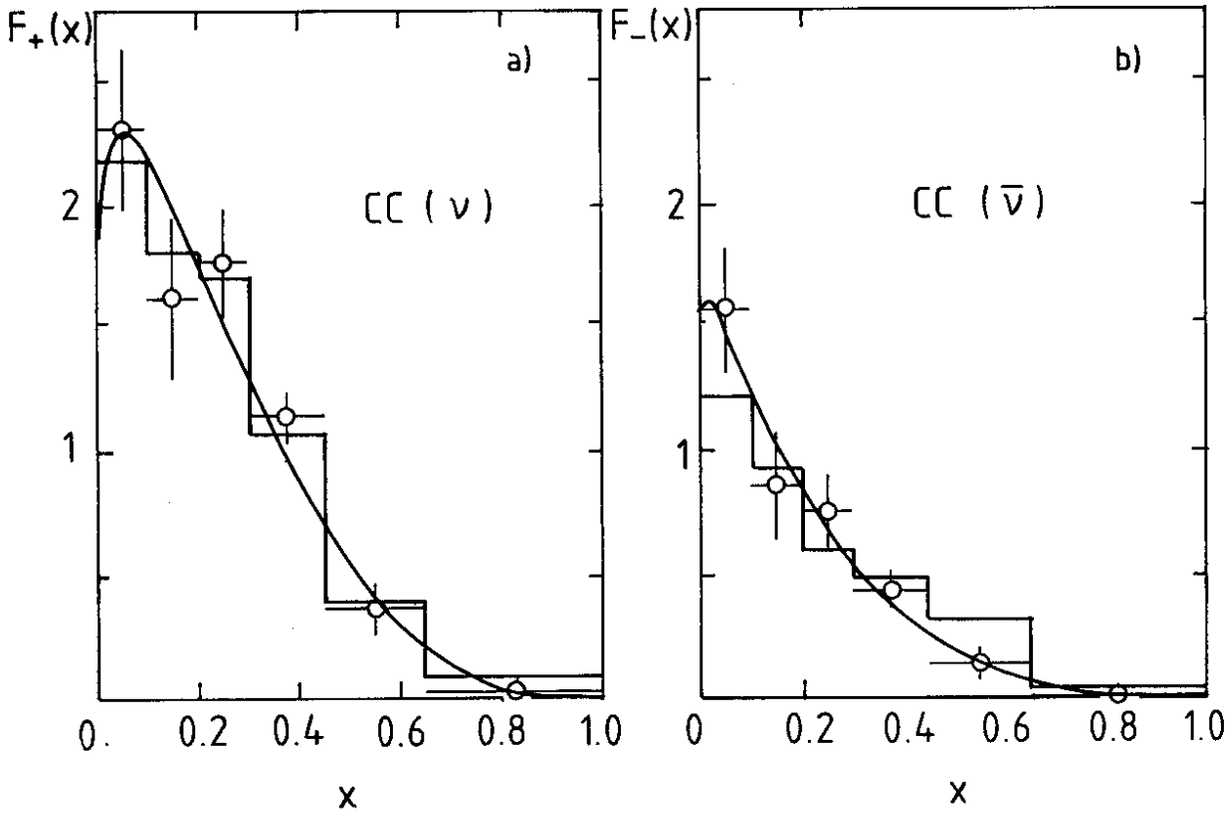
F+(x)
a)
CC (ν)
F_(x)
b)
CC (ν̄)
2
1
0.
0.2
0.4
0.6
0.8
1.0
x

Fig. 1

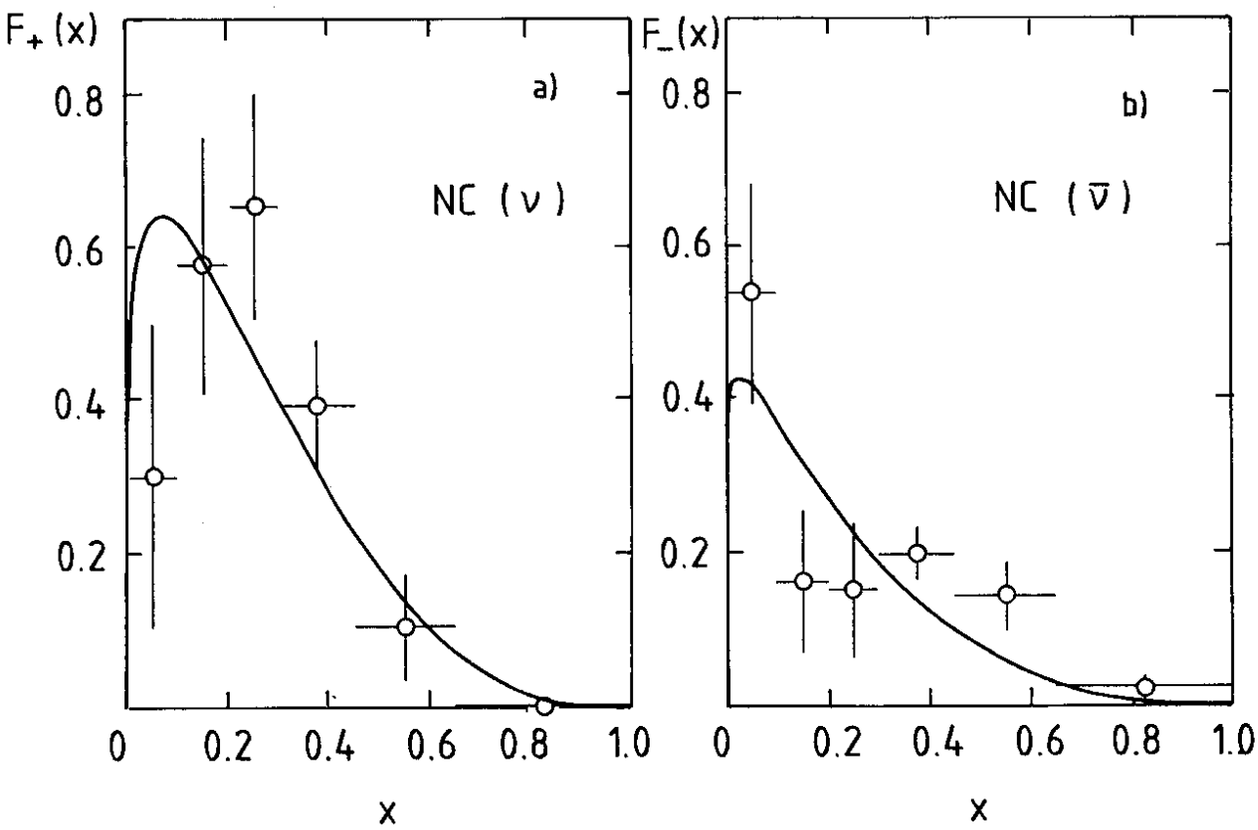
F+(x)
a)
NC (ν)
F_(x)
b)
NC (ν̄)
0.8
0.6
0.4
0.2
0
0.2
0.4
0.6
0.8
1.0
x

Fig. 2

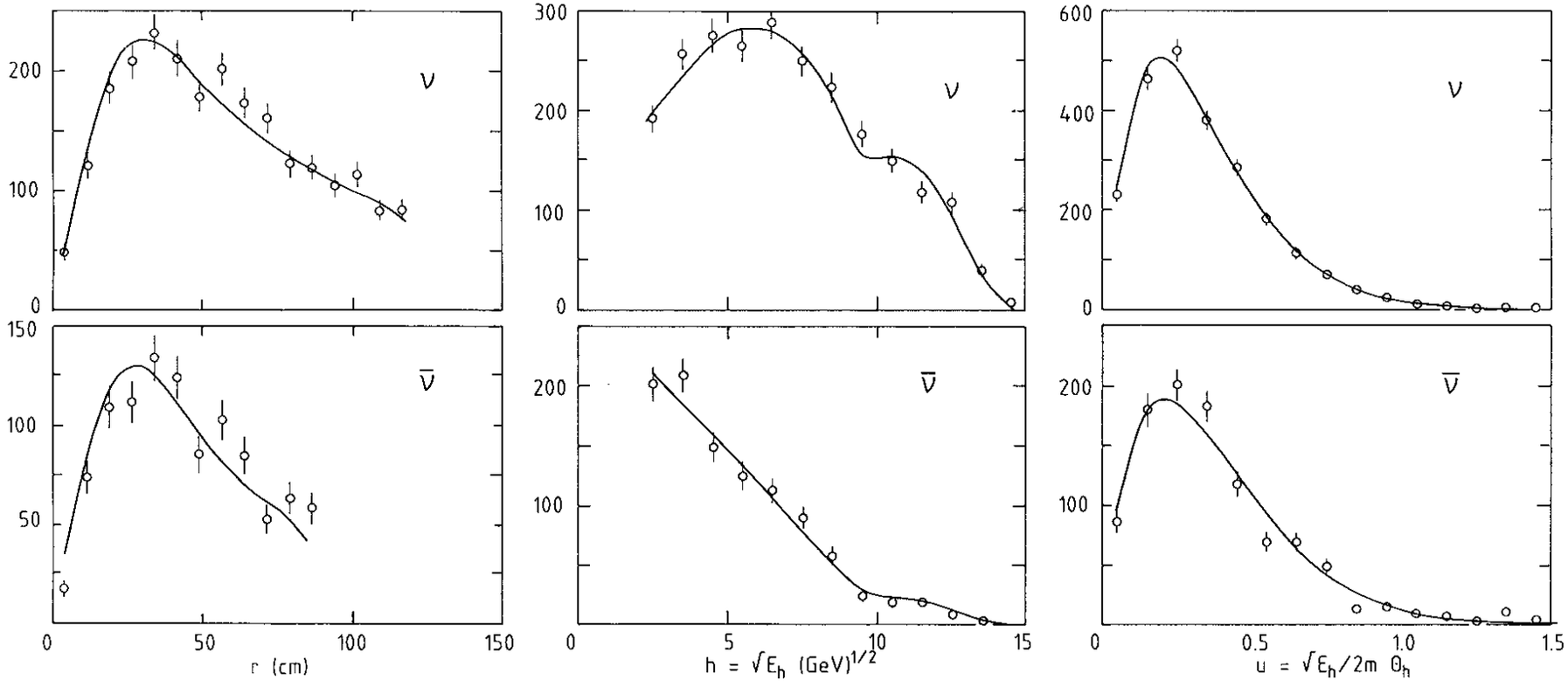

Fig. 3